Unsupervised Change Detection With Expectation-Maximization-Based Level Set

Ming Hao, Wenzhong Shi, Hua Zhang, and Chang Li

***Abstract*—The level set method, because of its implicit handling of topological changes and low sensitivity to noise, is one of the most effective unsupervised change detection techniques for remotely sensed images. In this letter, an expectation-maximization-based level set method (EMLS) is proposed to detect changes. First, the distribution of the difference image generated from multitemporal images is supposed to satisfy Gaussian mixture model, and expectation-maximization (EM) is then used to estimate the mean values of changed and unchanged pixels in the difference image. Second, two new energy terms, based on the estimated means, are defined and added into the level set method to detect those changes without initial contours and improve final accuracy. Finally, the improved level set method is implemented to partition pixels into changed and unchanged pixels. Landsat and QuickBird images were tested, and experimental results confirm the EMLS effectiveness when compared to state-of-the-art unsupervised change detection methods.**

***Index Terms*—Expectation-maximization (EM), level set method, remote sensing, unsupervised change detection.**

I. Introduction

CHANGE detection, one of the most important research topics for remote sensing, is generally achieved by analyzing remotely sensed images acquired from the same geographical area at different times [1]–[3]. In the past three decades, a variety of change detection methods have been developed. Such methods can be grouped into supervised and unsupervised methods. Although the supervised methods have the advantages of identifying types of change, robustness to atmospheric and light condition, and also have the ability to process multisource images over unsupervised ones, unsupervised change detection techniques are more widely used because of the absence of ground reference [2]. Widely used unsupervised methods include image differencing, image rationing, image regression, change vector analysis (CVA), and principal component analysis (PCA) [2]–[4].

Manuscript received November 19, 2012; revised February 6, 2013; accepted March 5, 2013. Date of publication May 23, 2013; date of current version November 8, 2013. This work was supported in part by the Fundamental Research Funds for the Central Universities under Grant 2012LWB31, a Project Funded by the Priority Academic Program Development of Jainism Higher Education Institutions, and National Natural Science Foundation of China under Grants 41101407, 41201451.

M. Hao and H. Zhang are with the School of Environment Science and Spatial Informatics, China University of Mining and Technology, Xuzhou 221116, China.

W. Shi is with the Department of Land Surveying and Geo-informatics, The Hong Kong Polytechnic University, Hong Kong (e-mail: lswzshi@polyu.edu.hk).

C. Li is with the College of Urban and Environmental Science, Central China Normal University, Wuhan 430079, China.

Color versions of one or more of the figures in this paper are available online at http://ieeexplore.ieee.org.

Digital Object Identifier 10.1109/LGRS.2013.2252879

An active contour model (snakes) was proposed by Kass *et al.* [5], and Chan and Vese [6] improved this model with level set called the CV model. In recent years, active contour models based on level set are increasingly popular and used to process remotely sensed images [7]–[9]. In addition, the active contour model based on level set has also been used recently to detect changes for remotely sensed images [10], [11]. Initial contours, however, are needed to achieve accurate change-detection maps for the proposed method in [11]. In [12], the neighborhood distribution and edge information was derived by two localized region-based operators for each pixel, and then incorporated into a local binary fitting (LBF) as a local edge-based level set model. Selection of an initial contour in this model is not needed. In [13], a variational formulation, based on gradient, was added to the level set method. This forced the level set function to have the opposite sign along the edges at convergence. Hence, the improved level set achieved segmentation without initial contours.

This letter presents a novel approach to detect changes with expectation-maximization-based level set (EMLS) without initial contours. Firstly, the difference image distribution is assumed to satisfy the Gaussian mixture model, and the Expectation-Maximization (EM) is exploited to estimate the mean values of changed and unchanged pixels in the difference image. Two new energy terms are then added into the level set method, based on the mean values. Finally, the improved level set method is used to detect changes.

II. Methods

Generally, change detection can be seen as a classification problem for only two classes. Active contour models based on level set are widely used to segment images because of the advantages of implicit handling of topological changes, extraction of objects without noticeable edges, and low sensitivity to noise [6]. In [11], multiresolution level set (MLS) and MLS with the Kittler algorithm [14] (MLSK) were proposed to detect changes, and the results were satisfactory. However, MLS lacks stability when used for different types of changes and MLSK needs initial curves. To increase stability and achieve detection changes without initial contours, the mean values of changed and unchanged pixels, estimated by EM, are added into an active contour model.

Let X_1 and X_2 be two multispectral images acquired from the same geographical area at two different times. Assuming images have been co-registered and radiometrically corrected, the two images have the same size of $M \times N$. The difference

image X is generated by the magnitude of the CVA method, and consists of changed pixels W_1 and unchanged pixels W_2.

A. Estimation of the Mean Values by EM

In this paper, it is assumed that the difference image X can be seen as a Gaussian mixture, as follows:

$$p(X) = p(X/W_1)P(W_1) + p(X/W_2)P(W_2) \tag{1}$$

where $p(X)$, $p(X/W_1)$ and $p(X/W_2)$ are the probability density functions of the difference image X, changed pixels W_1 and unchanged pixels W_2, and $P(W_1)$ and $P(W_2)$ are the *a priori* probabilities of changed pixels and unchanged pixels, respectively. The probability density functions $p(X/W_1)$ and $p(X/W_2)$ are Gaussian and can be written as

$$p\left(X/W_k\right) = \frac{1}{\sigma_k\sqrt{2\pi}} \exp\left[-\frac{(X-\mu_k)^2}{2\sigma_k^2}\right] \tag{2}$$

here, $k \in (1, 2)$, μ_k and σ_k are the respective mean and variance of the corresponding pixels of class W_k.

Given that, EM can be performed to estimate the mean values μ_k by the following three steps [2], [15].

Step 1) : Initialize the means μ_k, covariances σ_k and *a priori* probability $\mathrm{P}(W_k)$. A threshold d to the difference image was set to obtain the initial changed pixels and unchanged pixels. The threshold can be generated from an empirical equation written as

$$d = \mu_{\mathrm{X}} + R \cdot \sigma_{\mathrm{X}} \tag{3}$$

where R is a constant, μ_{X} and σ_{X} denote the respective mean and standard deviation of the difference image. The values of μ_k, σ_k and $\mathrm{P}(W_k)$ can then be computed from the classified pixels and regarded as the initial values to EM.

Step 2) : Expectation step. Equations (1) and (2) are used to evaluate the *a posterior* probability $\mathrm{P}(W_k/X)$ with (4), as follows:

$$P(W_k/x_i) = \frac{P(W_k)p(x_i/W_k)}{P(x_i)} \tag{4}$$

here, $1 \le i \le MN$ and x_i is the ith pixel of the difference image.

Step 3) : Maximization step. Re-estimate the parameters using the following equations:

$$P^{t+1}(W_k) = \frac{\sum_{i=1}^{MN} P^t(W_k/x_i)}{MN} \tag{5}$$

$$\mu_k^{t+1} = \frac{\sum_{i=1}^{MN} P^t(W_k/x_i)x_i}{\sum_{i=1}^{MN} P^t(W_k/x_i)} \tag{6}$$

$$(\sigma_k^2)^{t+1} = \frac{\sum_{i=1}^{MN} P^t(W_k/x_i)(x_i-\mu_k)^2}{\sum_{i=1}^{MN} P^t(W_k/x_i)} \tag{7}$$

where the superscripts t and $t+1$ are the current and next iterations, respectively.

The parameters are estimated by the steps above, and then checked for convergence. If the convergence criterion is not satisfied, repeat steps 2 and 3 until convergence is achieved. Finally, the mean values are estimated.

B. Change Detection by Level Set

The changed pixels in the difference image can be seen as the object and extracted by finding an optimal contour C by the energy functional given as [6], [11]

$$E(C) = \int_{I(C)} |x_i - c_1|^2\, dxdy + \int_{O(C)} |x_i - c_2|^2\, dxdy + v\,|C| \tag{8}$$

where $v > 0$ is a constant, C is the evolving contour, $I(C)$ represents the area inside the evolving contour and can be seen as changed, $O(C)$ denotes the area outside the evolving contour and can be regarded as unchanged, $|C|$ denotes the length of the evolving contour, x_i is the ith pixel value of the difference image, c_1 and c_2 are the respective gray average of all pixels inside and outside the contour C. The term $\int_{I(C)} |x_i - c_1|^2\, dxdy$ is a sum of the differences between pixel gray values inside the contour C and the their corresponding mean value. Similarly, the term $\int_{O(C)} |x_i - c_2|^2\, dxdy$ is a sum of the differences between pixel gray values outside the contour C and their corresponding mean value. The contour then evolves in order to fit the edges of objects by making (8) reach a minimum value. Finally, the image is segmented into changed and unchanged parts, each with homogeneous pixels.

In [12] and [16], EM was embedded directly into the level set method for segmentation and object extraction. To get out of the need for initial contours and increase the correctness of change detections with the level set, two new terms are added into (8). This denotes the differences between the pixels of the difference image and the means of changed and unchanged pixels estimated by EM. The new equation can be written as [7]

$$\begin{aligned} E(C) = {} & \textstyle\int_{I(C)} |x_i - c_1|^2\, dxdy + \int_{O(C)} |x_i - c_2|^2\, dxdy \\ & + v\,|C| + \textstyle\int_{I(C)} |x_i - \mu_1|^2\, dxdy + \int_{O(C)} |x_i - \mu_2|^2\, dxdy \end{aligned} \tag{9}$$

here, μ_1 and μ_2 are the means of changed and unchanged parts in the difference image, respectively. The term $\int_{I(C)} |x_i - \mu_1|^2\, dxdy$ means a sum of the differences between pixel gray values inside the contour C and the mean value of changed pixels. Similarly, the term $\int_{O(C)} |x_i - \mu_2|^2\, dxdy$ is a sum of the differences between pixel gray values outside the contour C and mean value of unchanged pixels. The two terms can verify that the changed and unchanged pixels are detected correctly without initial contours and improve the distinguishability between changed and unchanged pixels.

To minimize the energy function (9), the level set method is exploited [17]. In the level set method, Ω represents the image domain and the curve C is represented by the zero level set of Lipchitz function φ, such that

$$\begin{cases} \varphi(x, y) > 0 & (x, y) \in I(C) \\ \varphi(x, y) = 0 & (x, y) \in C \\ \varphi(x, y) < 0 & (x, y) \in O(C) \end{cases}. \tag{10}$$

The Heaviside step function H and Dirac delta function δ are then introduced to describe the functional as follows:

$$H(z) = \begin{cases} 1 & z \geq 0 \\ 0 & z < 0 \end{cases}, \quad \delta(z) = \frac{d}{dz} H(z). \tag{11}$$

The energy function can be described using level set function φ instead of unknown variable C, and (9) can be written as

$$E(\varphi) = \int_{\Omega} |x_i - c_1|^2 H(\varphi) dxdy + \int_{\Omega} |x_i - c_2|^2 (1 - H(\varphi)) dxdy + v \int_{\Omega} \delta(\varphi) |\nabla \varphi| \, dxdy + \int_{\Omega} |x_i - \mu_1|^2 H(\varphi) dxdy + \int_{\Omega} |x_i - \mu_2|^2 (1 - H(\varphi)) dxdy \tag{12}$$

here, $\nabla\varphi$ means the gradient of φ. To obtain a global minimizer, the functions H and δ are replaced by the regularized versions as

$$H_\varepsilon(z) = \frac{1}{2}\left(1 + \frac{2}{\pi} \arctan\left(\frac{z}{\varepsilon}\right)\right), \quad \delta_\varepsilon(z) = \frac{1}{\pi} \frac{\varepsilon}{\varepsilon^2 + z^2}. \tag{13}$$

Based on the above, the next steps are implemented iteratively until the optimal φ is obtained [6].

Keeping φ fixed, the energy functional is minimized with respect to c_1 and c_2, and they can be obtained by

$$c_1 = \frac{\int_\Omega x_i H(\varphi) dxdy}{\int_\Omega H(\varphi) dxdy} \tag{14}$$

$$c_2 = \frac{\int_\Omega x_i (1 - H(\varphi)) dxdy}{\int_\Omega (1 - H(\varphi)) dxdy}. \tag{15}$$

Keeping c_1 and c_2 fixed, the energy functional is minimized with respect to φ. The associated Euler–Lagrange equation parameterizing the descent direction by an artificial time t ($t \geq 0$) is given as

$$\frac{\partial \varphi}{\partial t} = \delta_\varepsilon(\varphi) \left[v \operatorname{div}\left(\nabla\varphi / |\nabla\varphi|\right) - |x_i - c_1|^2 + |x_i - c_2|^2 - |x_i - \mu_1|^2 + |x_i - \mu_2|^2 \right]. \tag{16}$$

A finite differences implicit scheme is then used to discretize the equation and achieve the solution of the evolution equation in φ. More details about numerical approximation are given in [6].

III. Experimental Results

To evaluate the EMLS performance for change detection, two remotely sensed image data sets were tested. Three indexes are used to assess the results [18]: 1) miss detection (MD): the number of unchanged pixels in the changed detection map, incorrectly classified when compared to the ground reference map. The miss detection rate P_m is calculated by the ratio $P_\mathrm{m} = MD/N_0 \times 100\%$, here, N_0 is the total number of changed pixels counted in the ground reference map, 2) false alarm (FA): the number of changed pixels in the change detection map incorrectly classified when compared to the ground reference. The false detection rate P_f is described by the ratio $P_\mathrm{f} = FA/N_1 \times 100\%$, where N_1 is the total number of unchanged pixels counted in the ground reference map, and 3) total error (TE): the total number of detection errors, including both miss and false detections, which is the sum of the FA and the MD. Hence, the total error rate P_t is described by $P_\mathrm{t} = (FA + MD)/(N_0 + N_1) \times 100\%$.

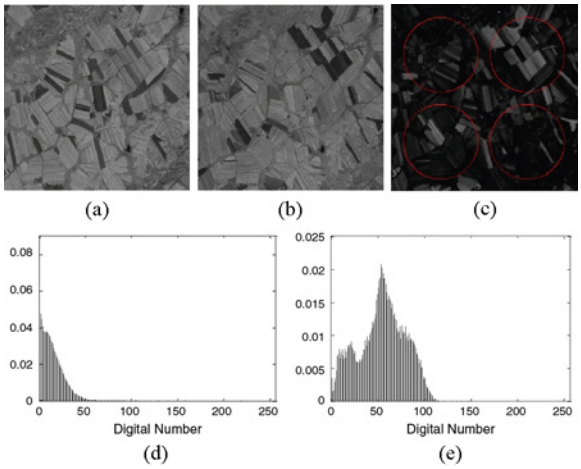

Fig. 1. Data set 1 acquired by ETM+ sensor in (a) August 2001 and (b) August 2002. (c) Difference image with initial curves. (d) Histogram of the unchanged pixels. (e) Histogram of the changed pixels.

In addition, to avoid being trapped into a local minimum, the multiresolution analysis in [11] is also employed in EMLS. The multiresolution images are generated by resizing the difference image with a factor 0.25, 0.5, and 1. The proposed method is then utilized from the coarse to fine resolution image. Referencing literature dealing with level set change detection [11] and segmentation and considering the data sets used in our experiments, $v = 0.1$ is a relatively reasonable empirical value for change detection. In addition, the time step Δt is set to 0.1 as used in [5] and [11]. The proposed EMLS is compared with robust level set methods LSII [19], MRSFE [20], DRLSE [21], CV, MLS, and MLSK to prove the effectiveness of EMLS. All the experiments were implemented on a personal computer with a 2.0 GHz CPU and 4.00 GB RAM.

A. Experiments on the Data Set 1

The first data set used in the experiments includes two multispectral images of size 400×400 pixels acquired by the Landsat-7 enhanced thematic mapper plus (ETM+) sensor in August 2001 (t1) and August 2002 (t2) in the Liaoning Province of China. Fig. 1(a) and (b) shows the band 4 of t1 and t2 images, respectively. The t1 image was registered to t2 image and the histogram matching method was used to both images for the relative radiometric correction. A mean filtering (3×3 window size) was applied to both images. The difference image was then generated by the CVA method.

Based on the above, EM was utilized to evaluate the means μ_1 and μ_2 of changed and unchanged pixels. The value of R is used ranging from -1 to 1 with 0.5 steps to discuss the effects of different initialization on the estimated mean values. The estimated mean values are presented in Table I. It is indicated that the mean values were accurately estimated by comparison with the histograms of changed and unchanged pixels in Fig. 1. In addition, it is important to point out that the stability of the estimation versus the various values of the initialization parameter d.

TABLE I
ESTIMATED MEAN VALUES OF THE CHANGED AND UNCHANGED PIXELS FOR DIFFERENT INITIALIZATION OF DATA SET 1

R	d	Initialization		Estimation	
		μ_1	μ_2	μ_1	μ_2
−1	−0.8	–	–	–	–
−0.5	10.1	32.2	4.4	46.2	13.5
0	21.0	45.3	8.8	46.2	13.5
0.5	31.9	56.7	11.5	46.3	13.5
1	42.9	65.2	13.3	46.3	13.5

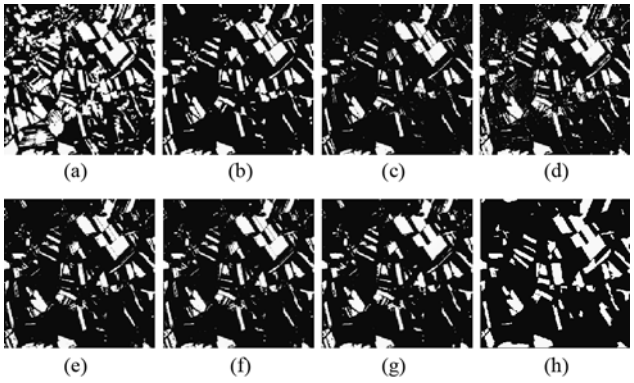

Fig. 2. Change detection results of data set 1 obtained by (a) LSII, (b) MRSFE, (c) DRLSE, (d) CV model, (e) MLS, (f) MLSK, (g) proposed EMLS, and (h) reference map.

TABLE II
ACCURACY INDEXES (P_m, P_f AND P_t) AND COMPUTATION TIME (SECOND) FOR DATA SET 1

Method	P_m(%)	P_f (%)	P_t (%)	T(s)
LSII	19.1	24.9	23.8	102.5
MRSFE	24.5	5.0	8.7	23.2
DRLSE	30.2	3.1	8.4	66.4
CV	20.8	7.6	10.1	25.3
MLS	26.0	3.8	8.0	9.7
MLSK	24.7	3.9	7.8	8.3
EMLS	**25.1**	**3.2**	**7.3**	**8.3**

The level set added the both mean values was applied to the difference image, where the initial curves were circles evenly covering the image shown in Fig. 1(c). From the conducted experiments, it is indicated that the number of initial curves does not affect the accuracy and computation time of the proposed method. Finally, four initial circles were adopted in this experiment.

Fig. 2 shows the best change detection results generated by LSII, MRSFE, and DRLSE. In addition, CV model, MLS, MLSK, and the proposed EMLS were implemented with the same parameters v=0.1 and Δt = 0.1. To assess the effectiveness of EMLS quantificationally, the three indexes, miss detection rate P_m, false detection rate P_f, and total error rate P_t, were computed based on change detection results and reference data, as depicted in Table II. The values of P_m, P_f, and P_t in EMLS were equal to 25.1%, 3.2%, and 7.3%, respectively. Compared to other methods, the proposed EMLS is more accurate in this experiment. It is worth noting that there is no need for the initial contours, indicating EMLS correctness. In terms of the computation times, the EMLS is similar to MLS and MLSK, but much faster than other methods, as shown in Table II.

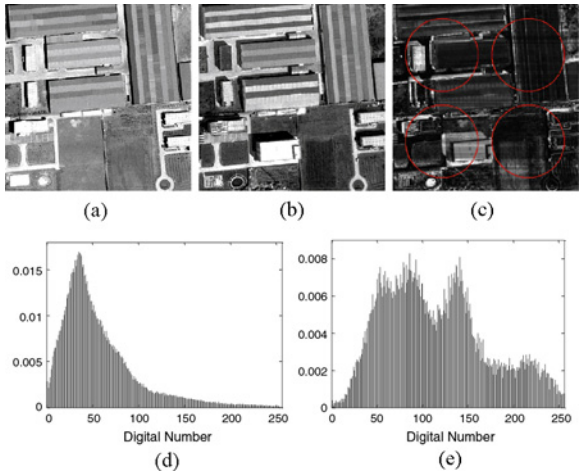

Fig. 3. Data set 2 acquired by the QuickBird sensor in (a) May 2005 and (b) March 2007, (c) difference image with initial curves, (d) histogram of the unchanged pixels, and (e) histogram of the changed pixels.

TABLE III
ESTIMATED MEAN VALUES OF THE CHANGED AND UNCHANGED PIXELS FOR DIFFERENT INITIALIZATION OF DATA SET 2

R	d	Initialized		Estimated	
		μ_1	μ_2	μ_1	μ_2
−1	15.0	68.4	9.2	114.9	40.7
−0.5	39.3	87.9	24.5	115.0	40.7
0	63.5	112.8	34.6	115.0	40.8
0.5	87.8	138.5	42.2	115.5	40.8
1	112.0	160.5	47.4	115.5	40.8

B. Experiments on the Data Set 2

The second data set consisted of QuickBird sensor images of size 512×512 pixels acquired in May 2005 (t1) and March 2007 (t2) in the Xuzhou Province of China. Fig. 3(a) and (b) shows t1 and t2 images, respectively. Both images were registered and the histogram matching method was used for the relative radiometric correction. Also, a mean filtering (3×3 window size) was implemented to both images. The difference image was then generated by the CVA method.

The EM method was applied to evaluate the means μ_1 and μ_2 of changed and unchanged pixels. The mean values were calculated with the various values of R ranging from −1 to 1 with the 0.5 steps and are presented in Table III. It can be seen that the mean values were accurately estimated when linked to the histograms of changed and unchanged pixels in Fig. 3. Additionally, the estimated mean values were still stable versus the various initializations.

The means μ_1 and μ_2 were added into the level set and it was used to detect changes in the difference image with the parameters v=0.1 and Δt = 0.1. The CV, MLS, and MLSK were also implemented to generate change detection maps with the same parameters in EMLS. In addition, LSII, MRSFE, and DRLS were performed to obtain best change detection maps and all changed maps are displayed in Fig. 4.

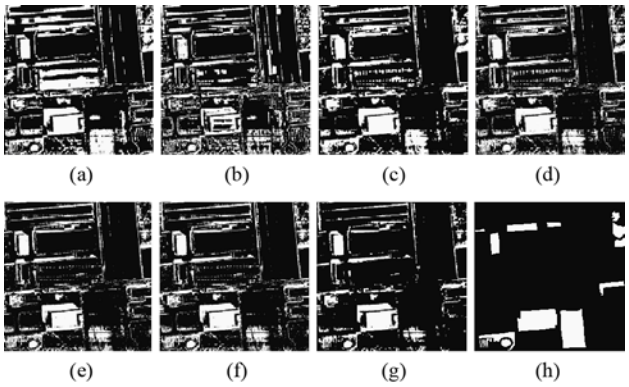

Fig. 4. Change detection results of data set 2 obtained by (a) LSII, (b) MRSFE, (c) DRLSE, (d) CV, (e) MLS, (f) MLSK, (g) proposed EMLS, and (h) reference map.

TABLE IV
ACCURACY INDEXES (P_m, P_f, AND P_t) AND COMPUTATION TIME (SECOND) FOR DATA SET 2

Method	P_m(%)	P_f (%)	P_t (%)	T(s)
LSII	31.1	24.9	25.7	175.7
MRSFE	49.5	23.3	26.4	46.2
DRLSE	30.9	18.1	19.6	67.8
CV	34.5	18.6	20.5	46.2
MLS	41.5	14.7	17.8	14.6
MLSK	40.7	15.0	18.0	17.0
EMLS	**48.2**	**9.3**	**14.1**	**13.9**

As shown in Fig. 4, it can be seen that the EMLS change map is the closest to the reference changes. The accuracy indexes were calculated based on the various change maps and the reference map shown in Table IV. The values of P_m, P_f, and P_t of EMLS are equal to 48.2%, 9.3%, and 14.1%. The accuracy of the proposed method is much more accurate than other methods. In terms of computation times, EMLS is the fastest in the seven methods. In addition, the proposed method can also detect changes accurately without initial curves.

IV. CONCLUSION

In this letter, an EMLS method was proposed to detect changes with remotely sensed images. Two new energy terms, denoting differences between pixels and the means of changed and unchanged pixels, were added into the initial level set to strengthen the correctness of the produced change maps. The main contribution of the proposed method was that initial contours were not needed. The effectiveness of the proposed EMLS was performed by Landsat and QuickBird images and the results showed that EMLS produces the most accurate change maps compared with those of LSII, MRSFE, DRLSE, CV, MLS, and MLSK.

As only the difference image was used in this letter, the errors caused by the difference image cannot be avoided. Hence, more information, such as correlation and texture information, may be fused by the level set method to improve the accuracy. This is worth further development.

ACKNOWLEDGMENT

The authors would like to thank the Editor and the four anonymous reviewers whose insightful suggestions have significantly improved this letter.

REFERENCES

[1] D. Lu, P. Mausel, E. Brondízio, and E. Moran, "Change detection techniques," *Int. J. Remote Sens.*, vol. 25, no. 12, pp. 2365–2401, Jun. 2004.
[2] L. Bruzzone and D. F. Prieto, "Automatic analysis of the difference image for unsupervised change detection," *IEEE Trans. Geosci. Remote Sens.*, vol. 38, no. 3, pp. 1171–1182, May 2000.
[3] P. Coppin, I. Jonckheere, K. Nackaerts, B. Muys, and E. Lambin, "Digital change detection methods in ecosystem monitoring: A review," *Int. J. Remote Sens.*, vol. 25, no. 9, pp. 1565–1596, May 2004.
[4] A. Singh, "Digital change detection techniques using remotely-sensed data," *Int. J. Remote Sens.*, vol. 10, no. 6, pp. 989–1003, 1989.
[5] M. Kass, A. Witkin, and D. Terzopoulos, "Snakes: Active contour models," *Int. J. Comput. Vision*, vol. 1, no. 4, pp. 321–331, 1988.
[6] T. F. Chan and L. A. Vese, "Active contours without edges," *IEEE Trans. Image Process.*, vol. 10, no. 2, pp. 266–277, Feb. 2001.
[7] S. Ahmadi, M. Zoej, H. Ebadi, H. A. Moghaddam, and A. Mohammadzadeh, "Automatic urban building boundary extraction from high resolution aerial images using an innovative model of active contours," *Int. J. Appl. Earth Observation*, vol. 12, no. 3, pp. 150–157, 2010.
[8] Y. Jing, J. An, and Z. Liu, "A Novel edge detection algorithm based on global minimization active contour model for oil slick infrared aerial image," *IEEE Trans. Geosci. Remote Sens.*, vol. 49, no. 6, pp. 2005–2013, Jun. 2011.
[9] J. Ball and L. Bruce, "Level set hyperspectral image classification using best band analysis," *IEEE Trans. Geosci. Remote Sens.*, vol. 45, no. 10, pp. 3022–3027, Oct. 2007.
[10] T. Celik and K. K. Ma, "Multitemporal image change detection using undecimated discrete wavelet transform and active contours," *IEEE Trans. Geosci. Remote Sens.*, vol. 49, no. 2, pp. 706–716, Feb. 2011.
[11] Y. Bazi, F. Melgani, and H. D. Al-Sharari, "Unsupervised change detection in multispectral remotely sensed imagery with level set methods," *IEEE Trans. Geosci. Remote Sens.*, vol. 48, no. 8, pp. 3178–3187, Aug. 2010.
[12] L. He, W. G. Wee, S. Zheng, and L. Wang, "A level set model without initial contour," in *Proc. Appl. Comp. Vision Workshop*, 2009, pp. 1–6.
[13] M. Li, C. He, and Y. Zhan, "Adaptive level-set evolution without initial contours for image segmentation," *J. Electron. Imaging*, vol. 20, no. 2, p. 023004, Apr.–Jun. 2011.
[14] J. Kittler and J. Illingworth, "Minimum error thresholding," *Pattern Recog.*, vol. 19, no. 1, pp. 41–47, 1986.
[15] C. M. Bishop, *Pattern Recognition Mach. Learning*. New York, NY, USA: Springer, 2006.
[16] T. F. Chan, H. Li, M. Lysaker, and X. C. Tai, "Level set method for positron emission tomography," *Int. J. Biomed. Imaging*, vol. 2007, p. 26950, 2007.
[17] S. Osher and J. A. Sethian, "Fronts propagating with curvature-dependent speed: Algorithms based on Hamilton–Jacobi formulations," *J. Comput. Phys.*, vol. 79, no. 1, pp. 12–49, 1988.
[18] Z. Yetgin, "Unsupervised change detection of satellite images using local gradual descent," *IEEE Trans. Geosci. Remote Sens.*, vol. 50, no. 5, pp. 1919–1929, May 2012.
[19] C. Li, R. Huang, Z. Ding, J. C. Gatenby, D. N. Metaxas, and J. C. Gore, "A level set method for image segmentation in the presence of intensity inhomogeneities with application to MRI," *IEEE Trans. Image Process.*, vol. 20, no. 7, pp. 2007–2016, Jul. 2011.
[20] C. Li, C. Y. Kao, J. C. Gore, and Z. Ding, "Minimization of region-scalable fitting energy for image segmentation," *IEEE Trans. Image Process.*, vol. 17, no. 10, pp. 1940–1949, Oct. 2008.
[21] C. Li, C. Xu, C. Gui, and M. D. Fox, "Distance regularized level set evolution and its application to image segmentation," *IEEE Trans. Image Processing*, vol. 19, no. 12, pp. 3243–3254, Dec. 2010.